

Remark on the generalized Riemann problem method for compressible fluid flows

Jiequan Li ^{*}, Zhongfeng Sun

Department of Mathematics, Capital Normal University, Northern Road 105, Western Ring 3, 100037 Beijing, PR China

Received 31 May 2006; received in revised form 16 August 2006; accepted 21 August 2006

Available online 18 October 2006

Abstract

The generalized Riemann problem (GRP) method was proposed for compressible fluid flows based on the Lagrangian formulation [M. Ben-Artzi, J. Falcovitz, A second-order Godunov-type scheme for compressible fluid dynamics, *J. Comput. Phys.*, 55(1) (1984) 1–32], and a direct Eulerian version was developed in [M. Ben-Artzi, J. Li, G. Warnecke, A direct Eulerian GRP scheme for compressible fluid flows, *J. Comput. Phys.*, 28 (2006) 19–43] by using the concept of Riemann invariants. The central feature of the GRP method is the resolution of centered rarefaction waves. In this note we show how to use the concept of Riemann invariants in order to resolve the rarefaction waves in the Lagrangian coordinate system and result in the GRP scheme.

© 2006 Elsevier Inc. All rights reserved.

Keywords: The generalized Riemann problem (GRP) method; Riemann invariants; Resolution of rarefaction waves

1. Introduction

The generalized Riemann problem (GRP) method was originally developed for compressible fluid dynamics [1], then had many applications, see [2–4] and references therein. The method was first formulated for the one dimensional system of an unsteady and inviscid flow in the Lagrangian coordinate system

$$\frac{\partial U}{\partial t} + \frac{\partial F(U)}{\partial x} = 0,$$
$$U = \begin{pmatrix} \tau \\ u \\ \frac{u^2}{2} + e \end{pmatrix}, \quad F(U) = \begin{pmatrix} -u \\ p \\ up \end{pmatrix}, \quad (1.1)$$

where (x, t) are Lagrangian coordinates; $\tau = \frac{1}{\rho}$ is the specific volume, and ρ, u, p are the density, velocity and pressure, respectively. The internal energy e is given by a state equation $p = p(\tau, e)$. The main feature of the

^{*} Corresponding author. Tel.: +86 10 68907074; fax: +86 10 68900950.
E-mail address: jiequan@mail.cnu.edu.cn (J. Li).

GRP method is to resolve centered rarefaction waves analytically. In [1] the centered rarefaction waves are resolved by tracing the primitives u and p .

In the context of compressible fluid flows or even hyperbolic conservation laws, the concept of Riemann invariants plays a very useful role [7] and has an analogue in the diagonalization process of linear hyperbolic systems. This concept was used in order to derive a direct Eulerian scheme [9,6], which avoids the passage from the Lagrangian to the Eulerian framework. This concept can also be extended to a more general setting of hyperbolic balance laws [5].

An important mathematical factor is the Riemann invariants associated with centered rarefaction waves remain regular up to the singularity point of the waves. This is related to the fact that a Riemann invariant is constant throughout the corresponding isentropic rarefaction wave. This regularity property of Riemann invariants is in contrast to the fact that the derivatives of flow variables τ , u and p are singular at the initial discontinuity. Furthermore, it is very natural in the process of acoustic approximation, which leads to L_1 or E_1 scheme in [4], and G_1 in [5] (the letters L , E and G are referred to the words ‘‘Lagrangian’’, ‘‘Eulerian’’ and ‘‘GRP’’, respectively).

In this note, we show how to use the Riemann invariants in order to resolve the centered rarefaction waves occurring in the generalized Riemann problem. While the final result coincides with the original GRP treatment [1], the method of derivation is straightforward and conforms to the application of Riemann invariants in a variety of other systems [9,5,6].

In order to make this paper somewhat self-contained, we recall some basic facts about (1.1) in Section 2, including the concept of Riemann invariants, characteristic coordinates and the machinery of the GRP method. In Section 3, we explain the analogue of Riemann invariants in an acoustic approximation. As a central ingredient, the resolution of centered rarefaction waves is obtained by directly using the Riemann invariants in Section 4. Then we summarize the result about the time derivatives of solutions used in the GRP method in Section 5 and present several examples in Section 6.

2. Riemann invariants, characteristic coordinates and the GRP method

In this section we recall the Riemann invariants and characteristic coordinates for (1.1) in order to resolve the centered rarefaction waves occurring in the generalized Riemann problem, we keep the notations in [1] or [5], which are listed at the end of this section for the reader’s easy reference. We rewrite (1.1), for smooth flows, in the following form:

$$\partial_t \tau - \partial_x u = 0, \quad \partial_t u + \partial_x p = 0, \quad \partial_t S = 0, \tag{2.1}$$

where τ is the specific volume, u the velocity, p the pressure and S the entropy related to the other variables through the second law of thermodynamics

$$de = TdS - pd\tau \tag{2.2}$$

and T is the temperature. Regard p as a function of τ and S , $p = p(\tau, S)$. Then the local sound speed c is given by $c^2 = -\tau^2 \cdot \frac{\partial p(\tau, S)}{\partial \tau}$. The system (1.1) or (2.1) possesses three eigenvalues,

$$\lambda_- = -c/\tau, \quad \lambda_0 = 0, \quad \lambda_+ = c/\tau. \tag{2.3}$$

Let us introduce variables ψ and ϕ

$$\psi = u - \int^\tau \frac{c(w, S)}{w} dw, \quad \phi = u + \int^\tau \frac{c(w, S)}{w} dw. \tag{2.4}$$

Then the Riemann invariants associated with λ_- , λ_0 and λ_+ are, respectively, see [7],

$$\lambda_- : (\psi, S); \quad \lambda_0 : (u, p); \quad \lambda_+ : (\phi, S). \tag{2.5}$$

We regard all thermodynamic variables p , T , e and c as functions of τ and S . Then in terms of total differentials we can write the Riemann invariants ϕ and ψ (as functions of u , τ , S) as,

$$d\psi = du - \frac{c}{\tau} d\tau + \frac{\partial \psi}{\partial S} dS = du + \frac{\tau}{c} dp + K(\tau, S) dS, \tag{2.6}$$

where since $\frac{\partial \psi}{\partial S} = -\int^\tau \frac{1}{w} \cdot \frac{\partial c(w,S)}{\partial S} dw$, we have

$$K(\tau, S) = -\frac{\tau}{c} \frac{\partial p}{\partial S} - \int^\tau \frac{1}{w} \cdot \frac{\partial c(w, S)}{\partial S} dw. \tag{2.7}$$

Recall [4, (4.67)] that along the characteristic $C_+ : x'(t) = \frac{c}{\tau}$, we have $du + \frac{c}{\tau} dp = 0$, so that in this direction we get

$$d\psi = K(\tau, S)dS \quad \text{along } C_+. \tag{2.8}$$

Observe that this can be further simplified if we note that, by $\partial_t S = 0$, we have,

$$dS = \frac{c}{\tau} \frac{\partial S}{\partial x} dt \quad \text{along } C_+. \tag{2.9}$$

Similarly, since $\frac{\partial \phi}{\partial S} = \int^\tau \frac{1}{w} \cdot \frac{\partial c(w,S)}{\partial S} dw$, we have

$$d\phi = -K(\tau, S)dS, \quad dS = -\frac{c}{\tau} \frac{\partial S}{\partial x} dt, \quad \text{along } C_- : x'(t) = -\frac{c}{\tau}. \tag{2.10}$$

In particular, in the important case of polytropic gases, we have

$$p = (\gamma - 1)e/\tau, \quad c^2 = \gamma p \tau, \quad \gamma > 1, \tag{2.11}$$

where e is a function of S alone. Then the Riemann invariants ψ, ϕ are

$$\psi = u + \frac{2c}{\gamma - 1}, \quad \phi = u - \frac{2c}{\gamma - 1}. \tag{2.12}$$

In this case, by using (2.7) and (2.2) we obtain

$$K(\tau, S) = \frac{\tau}{(\gamma - 1)c} \frac{\partial p}{\partial S} = \frac{T}{c}. \tag{2.13}$$

It follows that:

$$d\psi = du + \frac{\gamma\tau}{(\gamma - 1)c} dp + \frac{c}{(\gamma - 1)\tau} d\tau, \quad d\phi = du - \frac{\gamma\tau}{(\gamma - 1)c} dp - \frac{c}{(\gamma - 1)\tau} d\tau, \tag{2.14}$$

$$T dS = \frac{c^2}{(\gamma - 1)\tau} d\tau + \frac{\tau}{(\gamma - 1)} dp. \tag{2.15}$$

Now we establish characteristic coordinates (α, β) . They are defined in terms of the integral curves of the following differential equations,

$$\frac{dx}{dt} = \frac{c}{\tau}, \quad \frac{dx}{dt} = -\frac{c}{\tau}. \tag{2.16}$$

To be more specific, β is the initial value of the slope $-c/\tau$ at the singularity $(x, t) = (0, 0)$, and α for the transversal characteristic curves is the x -coordinate of the intersection point with the leading β -curve. For polytropic gases, they may be properly normalized, see (4.2) and (4.3) in Section 4. We illustrate this notation of characteristic coordinates in Fig. 2.1.

Then all flow variables τ, p, u, S, T can be viewed as functions of (α, β) . In particular, the Lagrangian coordinates (x, t) are regarded as functions of (α, β) ,

$$x = x(\alpha, \beta), \quad t = t(\alpha, \beta), \tag{2.17}$$

which satisfy

$$\frac{\partial x}{\partial \alpha} = -\frac{c}{\tau} \frac{\partial t}{\partial \alpha}, \quad \frac{\partial x}{\partial \beta} = \frac{c}{\tau} \frac{\partial t}{\partial \beta}. \tag{2.18}$$

Differentiating the first equation in (2.18) with respect to β , the second with respect to α and subtracting, we deduce that the function $t = t(\alpha, \beta)$ satisfies a second order equation,

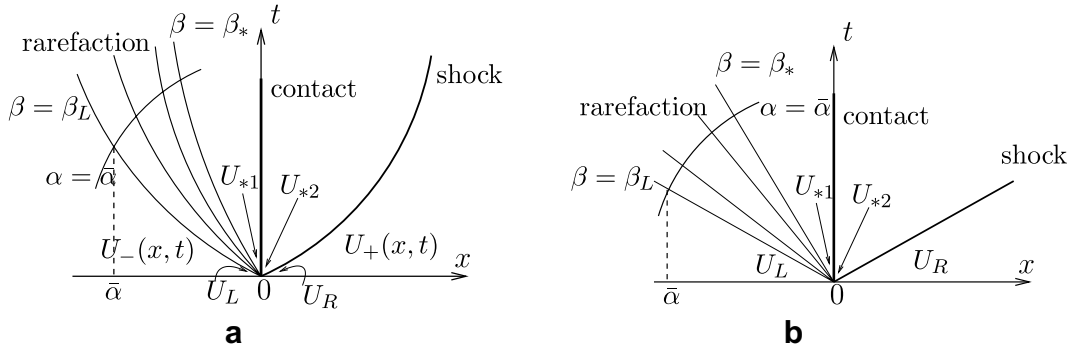


Fig. 2.1. A typical wave pattern for the generalized Riemann problem (1.1) and (2.23). (a) Wave pattern for the GRP. The initial data $U_0(x) = U_L + xU'_L$ for $x < 0$ and $U_0(x) = U_R + xU'_R$ for $x > 0$. (b) Wave pattern for the associated Riemann problem.

$$2 \frac{c}{\tau} \frac{\partial^2 t}{\partial \alpha \partial \beta} = - \frac{\partial(c/\tau)}{\partial \alpha} \cdot \frac{\partial t}{\partial \beta} + \frac{\partial(-c/\tau)}{\partial \beta} \cdot \frac{\partial t}{\partial \alpha}. \tag{2.19}$$

In terms of the characteristic coordinates (α, β) , we write the characteristic equations for ψ and S as,

$$\frac{\partial S}{\partial \beta} = \frac{\partial t}{\partial \beta} \cdot \frac{c}{\tau} \cdot S_x, \quad \frac{\partial \psi}{\partial \beta} = \frac{\partial t}{\partial \beta} \cdot \frac{c}{\tau} K(\tau, S) \cdot S_x, \tag{2.20}$$

where $S_x := \partial S / \partial x$ is regarded as a function of (α, β) . Denote

$$A(\alpha, \beta) = \frac{c(\alpha, \beta)}{\tau(\alpha, \beta)} K(\tau, S) \cdot S_x(\alpha, \beta). \tag{2.21}$$

Then ψ , as function of (α, β) , also satisfies a second order equation, after inserting (2.19),

$$\frac{\partial^2 \psi}{\partial \alpha \partial \beta} = \frac{\partial^2 t}{\partial \alpha \partial \beta} \cdot A + \frac{\partial t}{\partial \beta} \cdot \frac{\partial A}{\partial \alpha} = \frac{\tau}{2c} \cdot \frac{\partial t}{\partial \alpha} \cdot \frac{\partial(-c/\tau)}{\partial \beta} \cdot A + \frac{\partial t}{\partial \beta} \left[\frac{\partial A}{\partial \alpha} - \frac{\tau}{2c} \cdot \frac{\partial(c/\tau)}{\partial \alpha} \cdot A \right]. \tag{2.22}$$

This equation is very useful in the resolution of centered rarefaction waves.

Next we consider the generalized Riemann problem for (1.1) subject to the piecewise initial data

$$U(x, 0) = \begin{cases} U_L + U'_L x, & x < 0, \\ U_R + U'_R x, & x > 0. \end{cases} \tag{2.23}$$

The associated Riemann problem is the initial value problem for (1.1) with the piecewise constant value U_L and U_R (zero slopes in (2.23)). Denote the associated Riemann solution as $R^A(x/t; U_L, U_R)$, which can be obtained approximately or exactly, see [12]. The initial structure of the solution $U(x, t)$ to (1.1) and (2.23) is determined by the associated Riemann solution, and is described asymptotically as [10,11],

$$\lim_{t \rightarrow 0} U(\lambda t, t) = R^A(\lambda; U_L, U_R), \quad \lambda = x/t. \tag{2.24}$$

The local wave configuration is usually piecewise smooth and consists of rarefaction waves, shocks and contact discontinuities, as the schematic description in Fig. 2.1. The rarefaction wave as a part of the solution $R^A(x/t; U_L, U_R)$, is referred to as the associated rarefaction wave.

As is well known, the Riemann invariants remain constant across the corresponding associated rarefaction wave. For example, the functions ψ and S are invariant inside the associated rarefaction wave defined by the eigenvalue λ_- , as shown in Fig. 2.1(b). When the non-uniform initial data (2.23) is considered, the GRP solution of (1.1) can be regarded as the perturbation of $R^A(x/t; U_L, U_R)$. Therefore, ψ and S still remain regular inside the curved rarefaction wave (associated with λ_-) occurring the GRP solution. This fact motivates to use the Riemann invariants in resolving the rarefaction waves.

We are now in the position to explain the GRP method. As in [1,6], the GRP method consists of the following four steps.

Step 1. Given piecewise initial data

$$U^n(x) = U_j^n + \sigma_j^n(x - x_j), \quad x \in (x_{j-1/2}, x_{j+1/2}), \tag{2.25}$$

we solve the Riemann problem for (1.1) at each grid point $(x_{j+1/2}, t_n)$ to define the Riemann solution

$$U_{j+1/2}^n = R^\Lambda \left(0; U_j^n + \frac{\Delta x}{2} \sigma_j^n, U_{j+1}^n - \frac{\Delta x}{2} \sigma_{j+1}^n \right), \tag{2.26}$$

where σ_j^n and σ_{j+1}^n corresponds to U'_L and U'_R , respectively, in (2.23).

Step 2. Determine $(\partial U / \partial t)_{j+1/2}^n$ and calculate mid-point values $U_{j+1/2}^{n+1/2}$ approximately,

$$U_{j+1/2}^{n+1/2} = U_{j+1/2}^n + \frac{\Delta t}{2} \left(\frac{\partial U}{\partial t} \right)_{j+1/2}^n. \tag{2.27}$$

Step 3. Evaluate the new cell averages U_j^{n+1} using the updating formula,

$$U_j^{n+1} = U_j^n - \frac{\Delta t}{\Delta x} \left(F(U_{j+1/2}^{n+1/2}) - F(U_{j-1/2}^{n+1/2}) \right), \tag{2.28}$$

where F is the flux function in (1.1).

Step 4. Update the slope σ_j^{n+1} by the following procedure. Define

$$\begin{aligned} U_{j+1/2}^{n+1,-} &= U_{j+1/2}^n + \Delta t \left(\frac{\partial U}{\partial t} \right)_{j+1/2}^n, \\ \sigma_j^{n+1,-} &= \frac{1}{\Delta x} (\Delta U)_j^{n+1,-} := \frac{1}{\Delta x} \left(U_{j+1/2}^{n+1,-} - U_{j-1/2}^{n+1,-} \right). \end{aligned} \tag{2.29}$$

In order to suppress local oscillations near discontinuities, we apply to $\sigma_j^{n+1,-}$ a monotonicity algorithm-slope limiters,

$$\sigma_j^{n+1} = \text{minmod} \left(\epsilon \frac{U_j^{n+1} - U_{j-1}^{n+1}}{\Delta x}, \sigma_j^{n+1,-}, \epsilon \frac{U_{j+1}^{n+1} - U_j^{n+1}}{\Delta x} \right), \tag{2.30}$$

where the parameter $\epsilon \in [0, 2)$.

We can see that once the Godunov scheme for (1.1) is assumed, our GRP scheme is just to obtain the time derivatives $(\partial U / \partial t)_{j+1/2}^n$ used in Step 2. This is the main task in the present paper. In Table 1, we list some notations often used in the present paper.

3. Acoustic approximation

When $U_L = U_R$ and $U'_L \neq U'_R$, only linear waves emanate from the origin and the acoustic case follows (Fig. 3.1). Then the GRP scheme becomes simple and is stated in the following theorem.

Theorem 3.1 (Acoustic case). *When $U_* = U_L = U_R$ and $U'_L \neq U'_R$, we have the acoustic case. $(\partial p / \partial t)_*$, $(\partial u / \partial t)_*$ and $(\partial \tau / \partial t)_*$ can be solved as*

$$\begin{aligned} \left(\frac{\partial u}{\partial t} \right)_* &= -\frac{1}{2} \left[p'_L + \frac{c_*}{\tau_*} u'_L + p'_R - \frac{c_*}{\tau_*} u'_R \right], \\ \left(\frac{\partial p}{\partial t} \right)_* &= -\frac{1}{2} \frac{c_*}{\tau_*} \left[p'_L + \frac{c_*}{\tau_*} u'_L - p'_R + \frac{c_*}{\tau_*} u'_R \right], \\ \left(\frac{\partial \tau}{\partial t} \right)_* &= -\frac{\tau_*^2}{c_*^2} \left(\frac{\partial p}{\partial t} \right)_*. \end{aligned} \tag{3.1}$$

Proof. We rewrite the first two equations of (1.1) as

$$p_t + \frac{c^2}{\tau^2} u_x = 0, \quad u_t + p_x = 0. \tag{3.2}$$

Table 1
Basic notations

Symbols	Definitions
τ, u, p, S	Specific volume, velocity, pressure, entropy
ψ, ϕ	Riemann invariants associated with $-c/\tau$ and c/τ , respectively
Q_L, Q_R	$\lim Q(x, 0)$ as $x \rightarrow 0_-, x \rightarrow 0_+$
Q'_L, Q'_R	Constants slope $\frac{\partial Q}{\partial x}$ for $x < 0, x > 0$
$R^\Lambda(\cdot; Q_L, Q_R)$	Solution of the Riemann problem subject to data Q_L, Q_R
Q_*	$R^\Lambda(0; Q_L, Q_R)$
Q_1, Q_2	The value of Q to the left, the right of contact discontinuity
$Q_-(x, t), Q_+(x, t)$	The solution in the left, the right
$\left(\frac{\partial Q}{\partial t}\right)_*$	$\frac{\partial Q}{\partial t}(x, t)$ at $x = 0$ as $t \rightarrow 0_+$
α, β	Two characteristic coordinates defined by c/τ and $-c/\tau$, respectively
σ_L, σ_R	Shock speed at time zero, corresponding to $-\frac{c}{\tau}, \frac{c}{\tau}$
$\mu^2 = \frac{\gamma-1}{\gamma+1}$	$\gamma > 1$ the polytropic index, $\gamma = 1.4$ for air

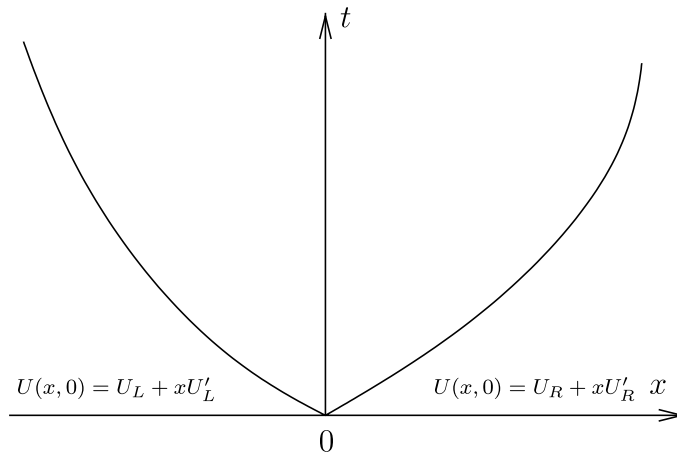


Fig. 3.1. The acoustic case: $U_L = U_R, U'_L \neq U'_R$.

We linearize this system around the state $U = U_*$ and use the standard diagonalization process to get

$$\left(u + \frac{\tau_*}{c_*} p\right)_t + \frac{c_*}{\tau_*} \left(u + \frac{\tau_*}{c_*} p\right)_x = 0, \quad \left(u - \frac{\tau_*}{c_*} p\right)_t - \frac{c_*}{\tau_*} \left(u - \frac{\tau_*}{c_*} p\right)_x = 0. \tag{3.3}$$

Then we find that

$$\left(\frac{\partial u}{\partial t}\right)_* + \frac{\tau_*}{c_*} \left(\frac{\partial p}{\partial t}\right)_* = -\frac{c_*}{\tau_*} u'_L - p'_L, \quad \left(\frac{\partial u}{\partial t}\right)_* - \frac{\tau_*}{c_*} \left(\frac{\partial p}{\partial t}\right)_* = \frac{c_*}{\tau_*} u'_R - p'_R, \tag{3.4}$$

which immediately gives $(\partial u/\partial t)_*$ and $(\partial p/\partial t)_*$ in (3.1).

For the computation of $(\partial \tau/\partial t)_*$, we use the following identity, which is obtained from the equation of state $p = p(\tau, S)$ and the entropy equation $\frac{\partial S}{\partial t} = 0$,

$$\frac{\partial p}{\partial t} = -\frac{c^2}{\tau^2} \frac{\partial \tau}{\partial t} + \frac{\partial p}{\partial S}(\tau, S) \cdot \frac{\partial S}{\partial t} = -\frac{c^2}{\tau^2} \frac{\partial \tau}{\partial t}. \quad \square \tag{3.5}$$

Remark 3.2. The quantities $u + \frac{\tau}{c_*} p$ and $u - \frac{\tau}{c_*} p$ are the Riemann invariants in the acoustic case. This motivates us to use Riemann invariants in the resolution of centered rarefaction waves.

Remark 3.3. In the implementation of the GRP method, we use the acoustic approximation when $|U_L - U_R| \ll 1$. In fact, most cases involve this approximation.

4. The resolution of centered rarefaction waves

In this section we use the Riemann invariants as the main variables to resolve the centered rarefaction waves occurring in the generalized Riemann problem (1.1) and (2.23), instead of tracing the singularity of flow variables u , p and τ .

Consider the rarefaction waves associated with $-\frac{c}{\tau}$ and denote by $U_-(x, t)$ (resp. $U_1(x, t)$) the states (regions of smooth flows) ahead (resp. behind) the rarefaction wave, see Fig. 2.1(a) where $U_-(x, t)$ is determined by the left initial data $U_L + U'_L x$. Characteristic curves throughout the rarefaction wave are denoted by $\beta(x, t) = \beta$ and $\alpha(x, t) = \alpha$, $\beta \in [\beta_L, \beta_*]$, $-\infty \leq \alpha < 0$, $\beta_L = -\frac{c_L}{\tau_L}$, $\beta_* = -\frac{c_*}{\tau_*}$. Here β and α are denoted as follows: β is the initial value of the slope $-\frac{c}{\tau}$ at the singularity $(x, t) = (0, 0)$, and α for the transversal characteristic curves is the x -coordinate of the intersection point with the leading β -curve, which may be properly normalized, see below for polytropic gases.

Since the initial structure of the solution to (1.1) and (2.23) is determined by the associated Riemann problem, the rarefaction wave in Fig. 2.1(a) is asymptotically the same as the associated rarefaction wave $R^A(x/t; U_L, U_R)$ in Fig. 2.1(b) at the origin. The latter is expressed by using

$$x/t = -c/\tau, \quad \psi = \text{const} = \psi_L, \quad S = S_L. \tag{4.1}$$

The characteristic coordinates inside this associated centered rarefaction wave are, see [4], after a normalization,

$$t_{\text{ass}}(\alpha, \beta) = \alpha(-\beta)^{-1/2}, \quad x_{\text{ass}}(\alpha, \beta) = -\alpha(-\beta)^{1/2}. \tag{4.2}$$

Note that now $\alpha > 0$. They are the leading terms, in terms of α , of the transform (2.17), as $\alpha \rightarrow 0$,

$$x(\alpha, \beta) = x_{\text{ass}}(\alpha, \beta) + O(\alpha^2), \quad t(\alpha, \beta) = t_{\text{ass}}(\alpha, \beta) + O(\alpha^2). \tag{4.3}$$

The following lemma resolves the centered rarefaction wave shown in Fig. 2.1(a). This result is the same as in [1].

Lemma 4.1. *The limiting values $\frac{\partial u}{\partial t}(0, \beta)$ and $\frac{\partial p}{\partial t}(0, \beta)$ satisfy the linear relation,*

$$a_L \frac{\partial u}{\partial t}(0, \beta) + b_L \frac{\partial p}{\partial t}(0, \beta) = d_L(\beta), \tag{4.4}$$

for all $\beta_L \leq \beta \leq \beta_*$, where

$$(a_L, b_L) = \left(1, \frac{\tau(0, \beta)}{c(0, \beta)} \right) \tag{4.5}$$

and $d_L = d_L(\beta)$ depends on the initial data U_L , U'_L and the Riemann solution $R^A(x/t; U_L, U_R)$. For polytropic gases, d_L is

$$d_L = \left[\frac{1 + \mu^2}{1 + 2\mu^2} \theta^{1/(2\mu^2)} + \frac{\mu^2}{1 + 2\mu^2} \theta^{(1+\mu^2)/\mu^2} \right] T_L S'_L / \tau_L - \theta^{1/(2\mu^2)} c_L / \tau_L \psi'_L, \quad \theta = c(0, \beta) / c_L, \tag{4.6}$$

Note that the limiting values $\tau(0, \beta)$, $c(0, \beta)$ are obtained from the associated Riemann solution $R^A(x/t; U_L, U_R)$, and $T_L S'_L$, ψ'_L are given by the formula (2.15) and (2.14), respectively.

Proof. The equation for ψ in (2.6) and the equation for S in (2.1) yield

$$\frac{\partial u}{\partial t} + \frac{\tau}{c} \frac{\partial p}{\partial t} = \frac{\partial \psi}{\partial t}. \tag{4.7}$$

Denote $\psi_\alpha(\alpha, \beta) = (\partial \psi / \partial \alpha)(0, \beta)$. Note that

$$\psi_\alpha = \frac{\partial t}{\partial \alpha} \cdot \left(\frac{\partial \psi}{\partial t} - \frac{c}{\tau} \frac{\partial \psi}{\partial x} \right). \tag{4.8}$$

Taking into account (2.8) and (2.9), we have

$$\frac{\partial \psi}{\partial t} + \frac{c}{\tau} \frac{\partial \psi}{\partial x} = \frac{c}{\tau} K(\tau, S) S_x, \tag{4.9}$$

so that for (4.8) we get

$$\frac{\partial \psi}{\partial t} = \frac{1}{2} \left[A(\alpha, \beta) + \psi_\alpha \cdot \left(\frac{\partial t}{\partial \alpha} \right)^{-1} \right], \tag{4.10}$$

(see (2.21) for the notation $A(\alpha, \beta)$). Hence Eq. (4.4) follows from (4.7) by setting $\alpha = 0$ and evaluating $\psi_\alpha(0, \beta)$ and $A(0, \beta)$.

- (i) *The computation of $A(0, \beta)$.* Note that the entropy function S is regular throughout the rarefaction wave. Then we use the entropy equation $\frac{\partial S}{\partial t} = 0$ to get

$$\frac{\partial}{\partial t} S_x = \frac{\partial}{\partial x} \frac{\partial S}{\partial t} = 0. \tag{4.11}$$

Denote $\bar{\alpha} = x(\alpha, \beta)$. Since $\alpha = \alpha(x, t)$ is chosen to be the x -coordinate of the intersection point of the C_+ -characteristic curve with the leading C_- -characteristic curve, we have $\alpha \geq \bar{\alpha} > 0$. In view that the points $(\bar{\alpha}, \beta_L)$ and (α, β) correspond to the same x -coordinate, we deduce from (4.11)

$$S_x(\alpha, \beta) = S_x(\bar{\alpha}, \beta_L). \tag{4.12}$$

It follows, by taking the limit $\alpha \rightarrow 0$, that:

$$S_x(0, \beta) = S_x(0, \beta_L) = S'_L. \tag{4.13}$$

Thus we conclude

$$A(0, \beta) = \frac{c(0, \beta)}{\tau(0, \beta)} K(\tau(0, \beta), S_L) S'_L. \tag{4.14}$$

Particularly, for the polytropic gases, we have, by using (2.13)

$$A(0, \beta) = \frac{T(0, \beta)}{\tau(0, \beta)} S'_L. \tag{4.15}$$

We use (2.2) and (2.11) to get $T/T_L = c^2/c_L^2$. Finally we obtain

$$A(0, \beta) = \theta^2 T_L S'_L / \tau(0, \beta) = \theta^{(1+\mu^2)/\mu^2} T_L S'_L / \tau_L, \tag{4.16}$$

where $\theta = c(0, \beta)/c_L$ and $T_L S'_L$ is given by (2.15).

- (ii) *The computation of $\psi_\alpha(0, \beta)$.* Note that $(\partial t / \partial \beta)(0, \beta) \equiv 0$. We set $\alpha = 0$ for (2.22) to obtain

$$\frac{\partial}{\partial \beta} \psi_\alpha(0, \beta) = \frac{\tau(0, \beta)}{2c(0, \beta)} \cdot \frac{\partial t_{\text{ass}}}{\partial \alpha}(0, \beta) \cdot A(0, \beta). \tag{4.17}$$

The integration from β_L to β gives

$$\psi_\alpha(0, \beta) = \psi_\alpha(0, \beta_L) + \int_{\beta_L}^{\beta} \frac{\tau(0, \xi)}{2c(0, \xi)} \cdot \frac{\partial t_{\text{ass}}}{\partial \alpha}(0, \xi) \cdot A(0, \xi) \, d\xi. \tag{4.18}$$

The initial data $\psi_\alpha(0, \beta_L)$ is obtained from (4.8) by setting $\beta = \beta_L$ and noting that $\frac{\partial \psi}{\partial x}(0, \beta_L) = \psi'_L$,

$$\psi_\alpha(0, \beta_L) = \frac{\partial t_{\text{ass}}}{\partial \alpha}(0, \beta_L) \left[A(0, \beta) - 2 \frac{c}{\tau} \frac{\partial \psi}{\partial x}(0, \beta) \right] \Big|_{\beta=\beta_L} = \left(\frac{c_L}{\tau_L} \right)^{1/2} (K(\tau_L, S_L) S'_L - 2\psi'_L). \tag{4.19}$$

For the polytropic gases, we obtain

$$\frac{\partial \psi}{\partial \alpha}(0, \beta) = \frac{\partial \psi}{\partial \alpha}(0, \beta_L) - B \left[\left(\frac{c}{c_L} \right)^{(1+2\mu^2)/2\mu^2} - 1 \right], \tag{4.20}$$

where

$$B = \frac{1}{1 + 2\mu^2} \cdot \frac{1}{(\tau_L c_L)^{1/2}} T_L S'_L. \tag{4.21}$$

Inserting (4.16) and (4.20) into (4.10) yields (4.6). \square

5. Time derivatives of solutions at the singularity

In order to derive the GRP scheme, we not only need to resolve the rarefaction wave, as did in Section 4, but the resolution of shocks also needs treating. For the latter, we can take the van Leer approach exactly, see [8], or refer to the original GRP paper [1]. The results are listed in Appendix A. Thus we have the following theorems.

Theorem 5.1 (Calculation of $(\partial p/\partial t)_*$ and $(\partial u/\partial t)_*$). *The limiting values $(\partial p/\partial t)_*$ and $(\partial u/\partial t)_*$ are obtained by solving a pair of linear algebraic equations*

$$\begin{aligned} a_L \left(\frac{\partial u}{\partial t} \right)_* + b_L \left(\frac{\partial p}{\partial t} \right)_* &= d_L, \\ a_R \left(\frac{\partial u}{\partial t} \right)_* + b_R \left(\frac{\partial p}{\partial t} \right)_* &= d_R, \end{aligned} \tag{5.1}$$

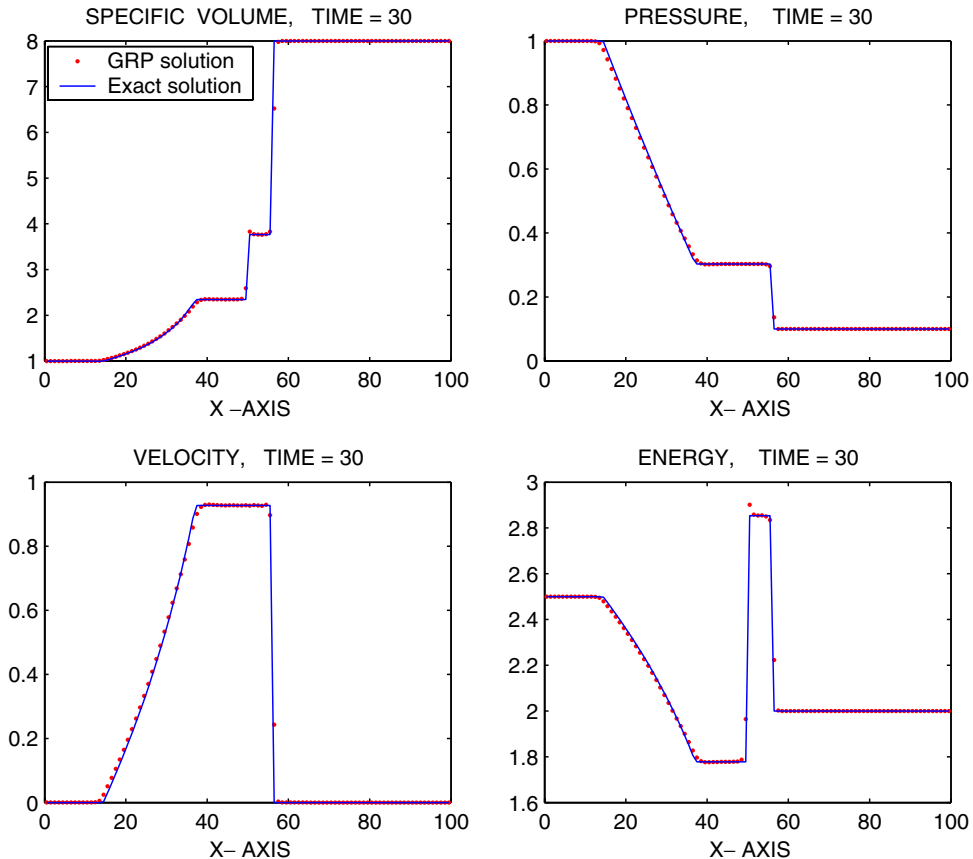


Fig. 6.1. Numerical results for Sod's problem: 100 grid points are used.

where a_L, a_R, b_L, b_R, d_L and d_R depends on the initial data (2.23) and the Riemann solution $R^\Lambda(0; U_L, U_R)$, and they are summarized in Appendix A.

Use the state equation $p = p(\tau, S)$ and the entropy equation $\frac{\partial S}{\partial t} = 0$. We see

$$\frac{\partial p}{\partial t} = \frac{\partial p}{\partial \tau} \cdot \frac{\partial \tau}{\partial t} + \frac{\partial p}{\partial S} \cdot \frac{\partial S}{\partial t} = -\frac{c^2}{\tau^2} \cdot \frac{\partial \tau}{\partial t}. \tag{5.2}$$

Noting that the specific volume τ and the sound speed c experience jumps across the contact discontinuity $x = 0$, $(\partial\tau/\partial t)_*$ is double-valued.

Theorem 5.2 (Calculation of $(\partial\tau/\partial t)_*$). *The limiting value $(\frac{\partial\tau}{\partial t})_*$ is calculated as follows:*

$$\left(\frac{\partial\tau}{\partial t}\right)_* = -\frac{\tau_*^2}{c_*^2} \left(\frac{\partial p}{\partial t}\right)_* \tag{5.3}$$

where τ_*, c_* can take either τ_{1*}, c_{1*} or τ_{2*}, c_{2*} .

6. Numerical examples

Once the generalized Riemann problem at each grid point is resolved, we can implement the GRP scheme following the steps in Section 2, see also [1,4,5]. In the choice of the parameter ϵ in the minmod limiter, we use $\epsilon = 1.9$. We choose the following three one-dimensional examples to illustrate the performance of the resulting scheme. The solid lines represent the exact solutions, while the dots stand for the corresponding GRP solutions.

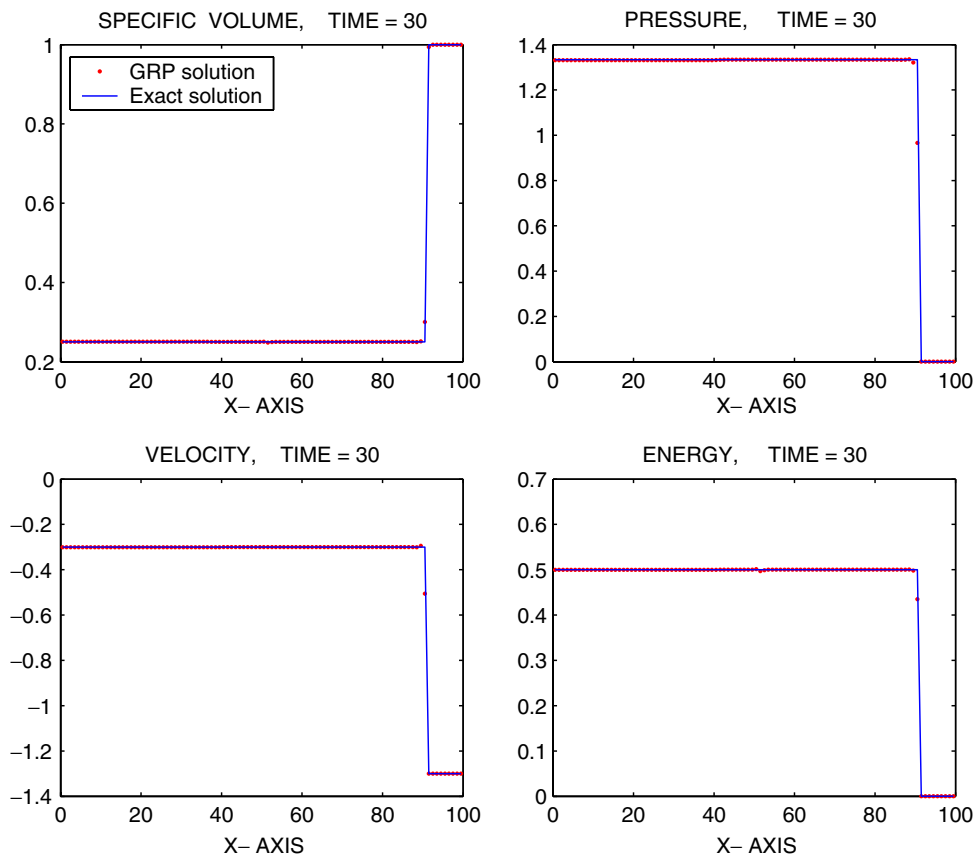


Fig. 6.2. Numerical results for a very strong nearly stationary shock: 100 grid points are used.

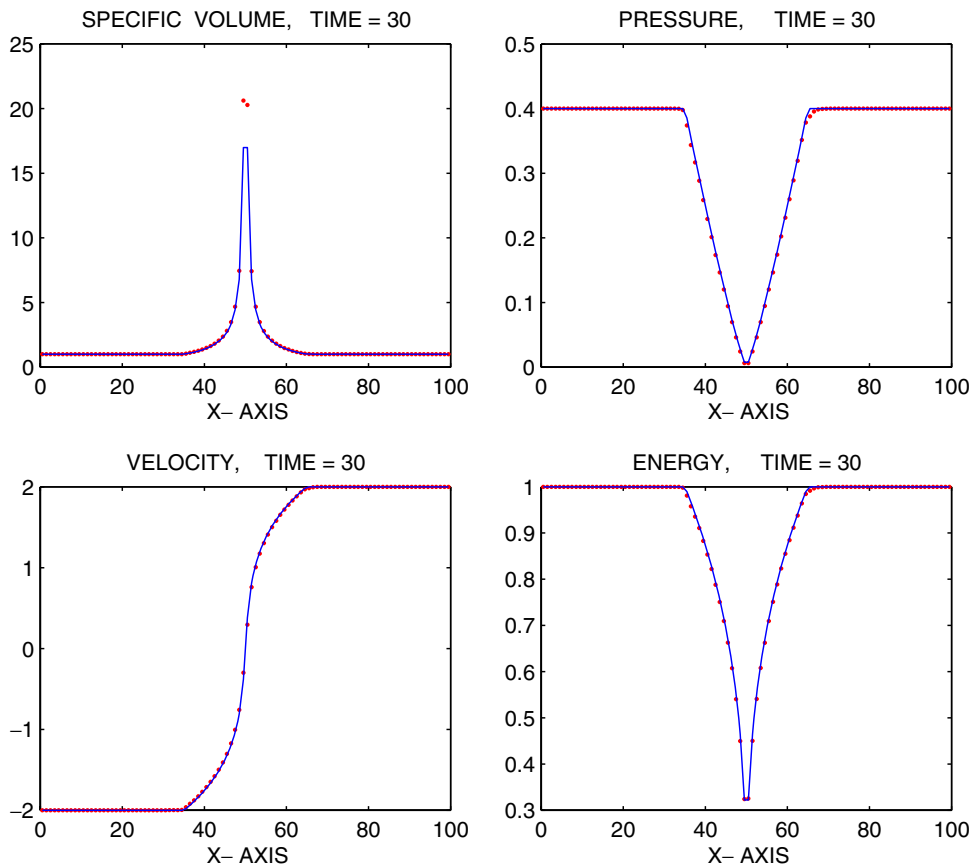


Fig. 6.3. Numerical results for the low density and energy problem: 100 grid points are used.

(a) *Sod problem.* As commonly used, our first example is the shock tube problem. The gas is initially at rest with $\tau = 1$, $p = 1$ for $0 \leq x \leq 50$ and $\tau = 8$, $p = 0.1$ for $50 < x \leq 100$. Numerical results are shown at time $t = 30$ in Fig. 6.1.

(b) *Nearly stationary shock.* Initially, $(\tau, u, p) = (0.25, -0.3, 4/3)$ for $0 \leq x \leq 50$ and $(\tau, u, p) = (1.0, -1.3, 10^{-6})$ for $50 < x \leq 100$. The polytropic index is taken to be $\gamma = 5/3$. The result is shown in Fig. 6.2.

(c) *Low density and internal energy Riemann problem.* The initial data is given with $(\rho, u, p) = (1, -2, 0.4)$ for $0 \leq x \leq 50$ and $(\rho, u, p) = (1, 2, 0.4)$ for $50 < x \leq 100$. The solid lines are obtained with the exact Riemann solvers in [4]. The dotted lines are obtained with 100 points. By this example we show that the GRP scheme can calculate low density problems and preserve the positivity of the density, pressure and energy to some extent although we cannot prove this property rigorously (Fig. 6.3).

Acknowledgments

Both authors appreciate the referee's careful remarks. The first author's research is supported by the grant NSFC with No. 10301022, the Natural Science Foundation from Beijing Municipality, Fok Ying Tong Education Foundation, the Key Program from Beijing Educational Commission with No. KZ200510028018, Program for New Century Excellent Talents in University (NCET) and Funding Project for Academic Human Resources Development in Institutions of Higher Learning Under the Jurisdiction of Beijing Municipality (PHR-IHLB).

Table 2
Useful coefficient for the GRP scheme

Two rarefaction waves	$(a_L, b_L) = (a_L^{\text{rare}}, b_L^{\text{rare}}), d_L = d_L^{\text{rare}}$ $(a_R, b_R) = (a_R^{\text{rare}}, b_R^{\text{rare}}), d_R = d_R^{\text{rare}}$
Two shocks	$(a_L, b_L) = (a_L^{\text{shock}}, b_L^{\text{shock}}), d_L = d_L^{\text{shock}}$ $(a_R, b_R) = (a_R^{\text{shock}}, b_R^{\text{shock}}), d_R = d_R^{\text{shock}}$
1-shock and 3-rarefaction wave	$(a_L, b_L) = (a_L^{\text{shock}}, b_L^{\text{shock}}), d_L = d_L^{\text{shock}}$ $(a_R, b_R) = (a_R^{\text{rare}}, b_R^{\text{rare}}), d_R = d_R^{\text{rare}}$
1-rarefaction wave and 3-shock	$(a_L, b_L) = (a_L^{\text{rare}}, b_L^{\text{rare}}), d_L = d_L^{\text{rare}}$ $(a_R, b_R) = (a_R^{\text{shock}}, b_R^{\text{shock}}), d_R = d_R^{\text{shock}}$

Appendix A. Useful coefficients for the GRP scheme

In Table 2, we collect for all cases the coefficients in Theorem 5.1 for the polytropic gases. The 1-shock (resp. 3-shock) refers to as the shock associated with the C_- family (resp. C_+ -family). Analogously for the 1-rarefaction wave and the 3-rarefaction wave.

The coefficients for rarefaction waves are given by

$$(a_L^{\text{rare}}, b_L^{\text{rare}}) = \left(1, \frac{\tau_{1*}}{c_{1*}}\right), \quad (a_R^{\text{rare}}, b_R^{\text{rare}}) = \left(1, -\frac{\tau_{2*}}{c_{2*}}\right), \tag{A.1}$$

$$d_L^{\text{rare}} = \left[\frac{1 + \mu^2}{1 + 2\mu^2} \left(\frac{c_{1*}}{c_L}\right)^{1/(2\mu^2)} + \frac{\mu^2}{1 + 2\mu^2} \left(\frac{c_{1*}}{c_L}\right)^{(1+\mu^2)/\mu^2} \right] T_L S'_L / \tau_L - \left(\frac{c_{1*}}{c_L}\right)^{1/(2\mu^2)} c_L \psi'_L / \tau_L, \tag{A.2}$$

$$d_R^{\text{rare}} = \left[\frac{1 + \mu^2}{1 + 2\mu^2} \left(\frac{c_{2*}}{c_R}\right)^{1/(2\mu^2)} + \frac{\mu^2}{1 + 2\mu^2} \left(\frac{c_{2*}}{c_R}\right)^{(1+\mu^2)/\mu^2} \right] T_R S'_R / \tau_R + \left(\frac{c_{2*}}{c_R}\right)^{1/(2\mu^2)} c_R \phi'_R / \tau_R. \tag{A.3}$$

The coefficients for shock waves are given by

$$a_L^{\text{shock}} = 1 - \Phi_1(p_*; p_L, \tau_L) \sigma_L, \quad b_L^{\text{shock}} = \Phi_1(p_*; p_L, \tau_L) - \sigma_L \frac{\tau_{1*}^2}{c_{1*}^2}, \tag{A.4}$$

$$d_L^{\text{shock}} = L_p^L \cdot p'_L + L_u^L \cdot u'_L + L_\tau^L \cdot \tau'_L, \tag{A.5}$$

$$a_R^{\text{shock}} = 1 + \Phi_1(p_*; p_R, \tau_R) \sigma_R, \quad b_R^{\text{shock}} = -\Phi_1(p_*; p_R, \tau_R) - \sigma_R \frac{\tau_{2*}^2}{c_{2*}^2}, \tag{A.6}$$

$$d_R^{\text{shock}} = L_p^R \cdot p'_R + L_u^R \cdot u'_R + L_\tau^R \cdot \tau'_R, \tag{A.7}$$

where all quantities involved are

$$L_p^L = -\sigma_L \Phi_2(p_*; p_L, \tau_L) - 1, \quad L_u^L = \sigma_L - \Phi_3(p_*; p_L, \tau_L) + \frac{c_L^2}{\tau_L^2} \Phi_2(p_*; p_L, \tau_L), \tag{A.8}$$

$$L_\tau^L = -\sigma_L \Phi_3(p_*; p_L, \tau_L), \quad \sigma_L = -\frac{u_* - u_L}{\tau_{1*} - \tau_L}, \tag{A.9}$$

$$L_p^R = \sigma_R \Phi_2(p_*; p_R, \tau_R) - 1, \quad L_u^R = \sigma_R + \Phi_3(p_*; p_R, \tau_R) - \frac{c_R^2}{\tau_R^2} \Phi_2(p_*; p_R, \tau_R), \tag{A.10}$$

$$L_\tau^R = \sigma_R \Phi_3(p_*; p_R, \tau_R), \quad \sigma_R = -\frac{u_* - u_R}{\tau_{2*} - \tau_R} \tag{A.11}$$

and (denote $(\bar{p}, \bar{\tau}) = (p_L, \tau_L)$ or $(\bar{p}, \bar{\tau}) = (p_R, \tau_R)$),

$$\begin{aligned} \Phi_1(p_*; \bar{p}, \bar{\tau}) &= \frac{1}{2} \sqrt{\frac{(1 - \mu^2)\bar{\tau}}{p_* + \mu^2\bar{p}}} \cdot \frac{p_* + (1 + 2\mu^2)\bar{p}}{p_* + \mu^2\bar{p}}, \\ \Phi_2(p_*; \bar{p}, \bar{\tau}) &= -\frac{1}{2} \sqrt{\frac{(1 - \mu^2)\bar{\tau}}{p_* + \mu^2\bar{p}}} \cdot \frac{(2 + \mu^2)p_* + \mu^2\bar{p}}{p_* + \mu^2\bar{p}}, \\ \Phi_3(p_*; \bar{p}, \bar{\tau}) &= \frac{p_* - \bar{p}}{2\bar{\tau}} \cdot \sqrt{\frac{(1 - \mu^2)\bar{\tau}}{p_* + \mu^2\bar{p}}}. \end{aligned} \tag{A.12}$$

References

- [1] M. Ben-Artzi, J. Falcovitz, A second-order Godunov-type scheme for compressible fluid dynamics, *J. Comput. Phys.* 55 (1) (1984) 1–32.
- [2] M. Ben-Artzi, J. Falcovitz, An upwind second-order scheme for compressible duct flows, *SIAM J. Sci. Statist. Comput.* 7 (3) (1986) 744–768.
- [3] M. Ben-Artzi, The generalized Riemann problem for reactive flows, *J. Comput. Phys.* 81 (1) (1989) 70–101.
- [4] M. Ben-Artzi, J. Falcovitz, *Generalized Riemann Problems in Computational Gas Dynamics*, Cambridge University Press, 2003.
- [5] M. Ben-Artzi, J. Li, Hyperbolic balance laws: Riemann invariants and the generalized Riemann problem, Preprint, 2006.
- [6] M. Ben-Artzi, J. Li, G. Warnecke, A direct Eulerian GRP scheme for compressible fluid flows, *J. Comput. Phys.* 28 (2006) 19–43.
- [7] C.M. Dafermos, *Hyperbolic Conservation Laws in Continuum Physics*, Springer, 2000.
- [8] B. van Leer, Towards the ultimate conservative difference scheme, V. A second-order sequel to Godunov’s method, *J. Comput. Phys.* 32 (1) (1979) 101–136.
- [9] Jiequan Li, Guoxian Chen, The generalized Riemann problem method for the shallow water equations with bottom topography, *Int. J. Numer. Methods Eng.* 65 (6) (2006) 834–862.
- [10] A. Bourgeade, Ph. LeFloch, P.-A. Raviart, An asymptotic expansion for the solution of the generalized Riemann problem. II. Application to the equations of gas dynamics, *Ann. Inst. H. Poincaré Anal. Non Linéaire* 6 (6) (1989) 437–480.
- [11] Ph. LeFloch, P.-A. Raviart, An asymptotic expansion for the solution of the generalized Riemann problem. I. General theory, *Ann. Inst. H. Poincaré Anal. Non Linéaire* 5 (2) (1988) 179–207.
- [12] E. Toro, *Riemann Solvers and Numerical Methods for Fluid Dynamics. A Practical Introduction*, Springer-Verlag, Berlin, 1997.